

Chapter 8

CARBON SEQUESTRATION FROM REMOTELY-SENSED NDVI AND NET ECOSYSTEM EXCHANGE

E. Raymond Hunt, Jr.

USDA ARS

Beltsville, Maryland

USA

J. T. Fahnestock

Robert D. Kelly

Jeffrey M. Welker

William A. Reiners

University of Wyoming

Laramie, Wyoming

USA

William K. Smith

Wake Forest University

Winston-Salem, NC

USA

ABSTRACT

Aircraft eddy flux measurements of net ecosystem exchange were acquired in 1999 over four southeastern Wyoming landscapes: a coniferous forest, a mixed dryland/irrigated agricultural area, a mixed-grass prairie, and a sagebrush steppe. A linear relationship between net ecosystem exchange and the absorbed photosynthetically active radiation was used to determine the efficiency of radiation use, which was used with remotely-sensed normalized difference vegetation index to calculate gross primary production. Chamber measurements of total ecosystem respiration for the sagebrush and grassland sites were used to develop a functional relationship with daily average temperature. The sagebrush and forest sites were net carbon sinks, whereas the grassland and agricultural sites were in carbon balance. Combining the use of remote sensing with net ecosystem exchange measurements avoids problems associated with small-scale flux sampling to determine areas of carbon sequestration. With large areas of the globe covered by rangelands, the potential for carbon sequestration may be significant.

R. S. Muttiah (ed.), *From Laboratory Spectroscopy to Remotely Sensed Spectra of Terrestrial Ecosystems*, pp 161-174. 2002 Kluwer Academic Publishers, Dordrecht, Netherlands.

1. INTRODUCTION

Managers of natural resources may be asked to alter their practices in order to offset emissions from fossil fuels (Paustian et al., 1998; Follett et al., 2001). Small, cost-effective changes applied to large areas may result in significant amounts of CO₂ being removed from the atmosphere. As a baseline for future changes, estimates of current carbon sequestration for different landscapes are required, preferably over several years to account for natural climatic variability.

There are many methods to estimate carbon sequestration, each method has advantages and disadvantages. One methodology is the measurement of net ecosystem exchange (NEE) using techniques from small, enclosed chambers to eddy flux towers and aircraft. Advances in technology and theory (Goulden et al., 1996; Baldocchi et al., 1996) have led to international efforts such as the Ameriflux and Euroflux networks. Furthermore, there is an important effort for estimating net ecosystem exchange in different types of rangelands (Svejcar et al., 1997; Frank et al., 2001). A second methodology is the monitoring of vegetation from satellite sensors such as the Advanced Very High Resolution Radiometer (AVHRR) or Moderate Resolution Imaging Spectrometer using changes in the Normalized Difference Vegetation Index (NDVI). AVHRR NDVI data are available from the United States Geological Survey EROS Data Center for many years, although there are some problems and artifacts with these data (Gutman, 1991, 1999; Cihlar et al., 1997).

The idea of combining remotely-sensed and ecosystem-flux data has been discussed many times (Ruimy et al., 1995, 1996; Running et al., 1999). The study presented here starts from the idea that NDVI data can best be used to determine gross primary production (GPP) using models of radiation use efficiency (Prince and Goward, 1995; Ruimy et al., 1995; Waring et al., 1995; Landsberg and Waring, 1997; Goetz and Prince, 1999). Small-chamber flux data are used to estimate daily respiration from average air temperature for the sagebrush and grassland ecosystems. The difference between GPP and respiration is assumed to be the amount of carbon sequestered for that year.

2. METHODS

Four sites in southeastern Wyoming were selected for measurement of net ecosystem exchange using an aircraft: (a) a mixed-grass prairie site near Chugwater, (b) a sagebrush steppe site in the Shirley Basin, (c) a heavily managed coniferous forest site in the Medicine Bow National Forest near Fox Park, and (d) a mixed irrigated/dryland agricultural site near Torrington (Color Plate 6A). The exact areas

of the sites were defined as being within a border 2.5 km around the 20 to 25 km-long flightlines of the Wyoming King Air aircraft, which was assumed to be the footprint of an eddy-covariance flux measurement system in the airplane. In 1999, the sagebrush and grassland sites had the most overflights, whereas acquisitions over the agricultural area in the summertime were few because of power plant emissions upwind (Kelly et al., in review).

Intensive study sites were established near the flightline midpoints for the grassland and sagebrush sites. Transparent chambers were used to measure carbon exchange rates four to five times daily from 1998 through 1999 with 12 replications. After the net fluxes were measured, opaque chambers were placed over the same location and used to determine total respiration rate. All of the respiration measurements for a 24-hour period were averaged to obtain a daily rate. Because respiration rates are an exponential function of temperature, $\ln(\text{daily rate})$ was regressed versus average daily temperature, defined as the average of the minimum and maximum air temperatures.

AVHRR data were acquired from the United States Geological Survey EROS Data Center (Sioux Falls, SD) for 1995 through 1999. These data are similar to the Conterminous US AVHRR Data Sets (Eidenshink, 1992), with the exception that the composites for 1998 and 1999 were done weekly instead of biweekly. Coverage began in late March and finished in early November.

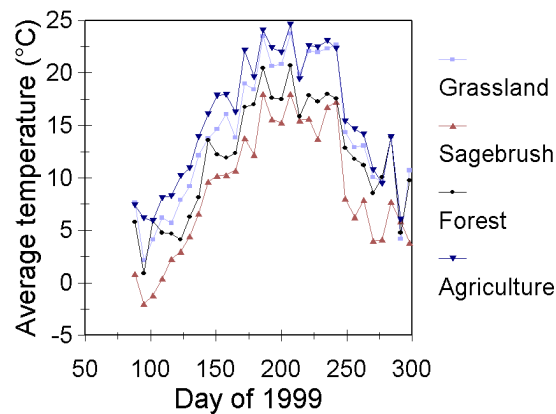


Figure 1. Average weekly temperatures for the four study sites in southeastern Wyoming.

For each composite period, the median value of NDVI was used from cloud-free images for the 120 to 150 1-km² pixels covering footprint of eddy-covariance system in the Wyoming King Air aircraft. For weekly composites from 1998 and 1999, there were many weeks with cloud cover affecting NDVI; thus, the average NDVI of the week before and after were used in place of the cloud-contaminated image.

Meteorological data were acquired from nearby National Weather Service stations for 1999. The average weekly temperatures are strongly related to site elevation (agriculture - 1312 m, grassland - 1693 m, sagebrush - 2184 m, and forest - 2732 m), except that the high-albedo sagebrush site was cooler than the low-albedo forest site (Fig. 1). Daily solar irradiances (MJ m⁻² day⁻¹) were calculated from the site meteorological data and from other stations around Wyoming using a model by Winslow et al. (in press). Incident photosynthetically active radiation (PAR, W m⁻²) were calculated from the weekly average solar irradiance multiplied by the fraction of PAR to solar radiation (measured to be 0.44 ± 0.04). Incident PAR was multiplied by the fraction of absorbed to incident PAR calculated from the NDVI data to determine the absorbed photosynthetically active radiation (APAR, MJ m⁻² day⁻¹). When NDVI data were not available (weeks 1-12 and 44-52), GPP was assumed to be zero.

3. RADIATION USE EFFICIENCY AND CARBON FLUXES

Radiation use efficiency is generally the amount of photosynthetic production per unit of radiation absorbed, with different operational definitions depending on specific situations and research objectives (Sinclair and Horie, 1989; Sinclair and Muchow, 1999). For this study, the efficiency of radiation use is defined as the mass of carbon uptake per absorbed photosynthetically active radiation (APAR). Following Ruimy et al. (1995), gross primary production (GPP, g C m⁻² time⁻¹) is summed over some time period from weekly to yearly:

$$GPP = \epsilon \sum APAR \quad [1]$$

where ϵ is the efficiency of radiation use (g C MJ⁻¹APAR) and APAR has units of MJ m⁻² day⁻¹. Often APAR is approximated by either intercepted PAR or intercepted solar radiation (Prince 1991; Running and Hunt 1993; Gower et al., 1999). Frequently, radiation use efficiency may be defined using the mass of dry matter rather than the mass of carbon, incorporating ash weight into the value of ϵ . Furthermore, radiation use efficiency is often determined using either net primary production or above-ground net primary production; thus, autotrophic respiration and carbon allocation are incorporated in the value of ϵ (Prince, 1991; Hunt and

Running, 1992; Running and Hunt, 1993; Hunt, 1994; Ruimy et al., 1994; Gower et al., 1999).

The maximum value of ϵ may be determined by the quantum yield of apparent photosynthesis, which is defined as the initial slope of leaf carbon exchange rate with respect to absorbed photosynthetic photon flux density. From the inverse of the quantum yield, the number of photons necessary to reduce one CO₂ molecule can be calculated (Table 1). The quantum yield of C₃ photosynthesis can vary between 0.03 and 0.08 mol CO₂ mol⁻¹ photons depending on conditions such as leaf temperature and ambient CO₂ concentration. By converting number of photons to radiant energy using Planck's Law, ϵ varies from about 1.7 to 4.4 g C MJ⁻¹ APAR (Table 1). Because the energy contained in a mol of photons is wavelength dependent, maximum ϵ may vary considerably under different environmental conditions.

Table 1. The efficiency of radiation use (ϵ) corresponding to different quantum yields of photosynthesis. Quantum yields are determined from the initial slope of leaf carbon exchange rate versus the absorbed photosynthetic photon flux density.

Quantum yield (mol CO ₂ mol ⁻¹ photons)	Photons/CO ₂	ϵ (g C MJ ⁻¹ APAR)
0.03	33.3	1.65
0.04	25.0	2.20
0.05	20.0	2.75
0.06	16.7	3.30
0.08	12.5	4.40

For actual growth conditions, ϵ will be reduced from the maximum because: stomatal closure caused by drought, high vapor pressure differences between leaf and air, night-time temperatures falling below freezing, ozone pollution, and other stresses affecting photosynthesis. Furthermore, Ruimy et al. (1995) concluded that ϵ is reduced, usually by about 50%, from the photosynthetic capacity of the foliage being light saturated (cf. Goetz and Prince, 1999).

3.1. Absorbed Photosynthetically Active Radiation

The direct physical quantity estimated from remotely-sensed NDVI is the fraction of absorbed to incident photosynthetically active radiation (f_{APAR} , dimensionless). The normalized difference vegetation index (NDVI) is defined:

$$\text{NDVI} = (\text{NIR} - \text{Red}) / (\text{NIR} + \text{Red}) \quad [2]$$

where NIR is the spectral radiance from a near-infrared band and Red is the spectral radiance from a red band. Originally, NDVI was developed to enhance the signal from vegetation and to reduce the effects of atmospheric transmittance, topography, and solar elevation and azimuth (Rouse et al., 1974). Subsequently, Asrar et al. (1984) and others showed that NDVI was approximately equal to f_{APAR} . AVHRR NDVI are most often used because these data are collected daily and composited over a short period, weekly or biweekly, to generate a mostly cloud-free image, so the change in f_{APAR} over a season may be determined.

Detailed canopy radiative transfer models are now used to relate f_{APAR} with NDVI from satellites (Baret and Guyot, 1991; Goward and Huemmrich, 1992; Ruimy et al., 1994; Myneni and Williams, 1994). For this study, the non-linear relationship between NDVI and f_{APAR} was linearly approximated:

$$f_{\text{APAR}} = 1.25 \text{ NDVI} - 0.10 \quad [3]$$

(Ruimy et al., 1994). The constant value of 0.10 was determined from the minimum value of AVHRR NDVI data during snow-free winter periods. Therefore, if ϵ is known, GPP can be calculated from meteorological data and remotely sensed NDVI:

$$\text{GPP} = \epsilon \sum n (1.25 \text{ NDVI} - 0.1) \text{ PAR} \quad [4]$$

where n is the number of days of the AVHRR compositing period and PAR is the mean daily incident photosynthetically active radiation over the same compositing period.

3.2. Net Ecosystem Exchange

Autotrophic respiration is the sum of all plant respiration, usually separated into growth and maintenance respiration. Heterotrophic respiration is the sum of respiration by animals, fungi and bacteria, and is most closely associated with the decomposition of organic matter. The relative contributions of autotrophic and heterotrophic respiration to the total are important, but cannot be separated using only soil-surface carbon exchange rates (Hanson et al., 2000). Net ecosystem exchange (NEE, $\text{g C m}^{-2} \text{ time}^{-1}$) is defined:

$$\text{NEE} = \text{GPP} - R_{\text{total}} \quad [5]$$

where R_{total} ($\text{g C m}^{-2} \text{ time}^{-1}$) is the sum of all autotrophic respiration and heterotrophic respiration over some time period. Replacing GPP in Equation [5], with Equation [1] above, leads to:

$$\text{NEE} = \epsilon \sum \text{APAR} - R_{\text{total}} \quad [6]$$

Equation [5] shows that when NEE is regressed versus $\sum \text{APAR}$ for short time intervals, the slope of the line should equal mean ϵ and the intercept should equal mean R_{total} (Ruimy et al., 1995). Thus, defining an RUE model on the basis of GPP, the main parameter ϵ can be estimated directly from net ecosystem exchange measurements.

The eddy-flux measurements were acquired from mid-morning to noon and represent the average of three to five overflights on a given day. NEE from the aircraft is linearly related to APAR (Fig. 2). The slope of the regression, ϵ was $0.51 \pm 0.07 \text{ g C MJ}^{-1} \text{ APAR}$ (slope \pm se), and the r^2 is 0.64. The slope of the regression for the forest site was $0.31 \pm 0.33 \text{ g C MJ}^{-1} \text{ APAR}$ based on only 7 points (not significantly different from a slope of zero). Using only four points of valid data, the slope of the regression for the agricultural site was $1.7 \pm 0.78 \text{ g C MJ}^{-1} \text{ APAR}$.

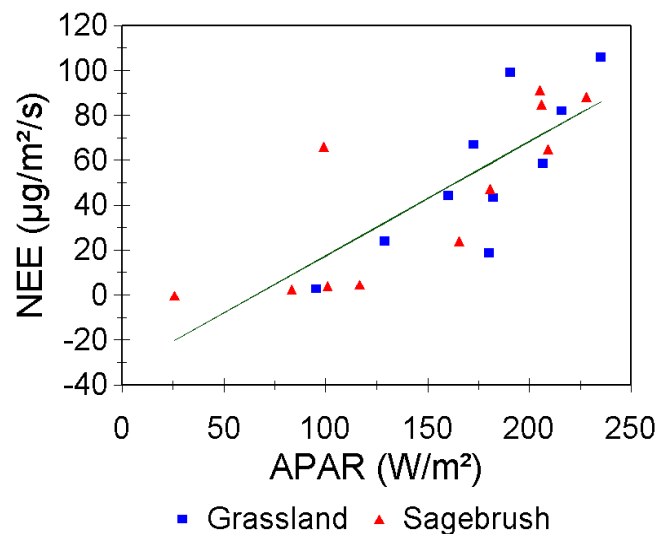


Figure 2. Relationship between instantaneous NEE measured by aircraft eddy flux techniques to APAR for the grassland and sagebrush sites.

There was no significant difference between ϵ among sites when tested using a dummy variable regression, so the data were combined. Because ϵ does not have units of time or area, the relationship between NEE and APAR presented in Eq. [6] may be scale independent.

3.3. Gross Primary Production Using Satellites

Using the mean ϵ of 0.51 g C MJ^{-1} APAR from the aircraft measurements for the four sites, GPP was estimated for each 1-km AVHRR pixel in the state of Wyoming (Color Plate 6B). Inspection of Color Plates 6A and 6B show that there are large variations in GPP for areas with the same lifeform. For example, sagebrush shrublands range from about 75 to $325 \text{ g C m}^{-2} \text{ year}^{-1}$ and forests range from about 275 to $525 \text{ g C m}^{-2} \text{ year}^{-1}$. Some of the range in GPP within a given lifeform is the result of the timing and amount of precipitation, which is the limiting environmental factor in Wyoming.

In addition, some of the range in GPP within a lifeform is the result of misclassification. GIS data from Driese et al. (1997) indicate that the landcover map in Color Plate 6A is only about 67% accurate, and there is considerable confusion between grassland and sagebrush shrubland areas. Yet it needs to be emphasized that these are not errors in GPP per se, because the aircraft NEE data indicates that for this study and location, there were no significant differences in ϵ among lifeforms (Fig. 2). Thus, Color Plate 6B shows a realistic representation of GPP over the different landscapes in the state of Wyoming.

4. RESPIRATION AND CARBON SEQUESTRATION

GPP is only part of the carbon cycle affecting carbon sequestration. Because mean R_{total} is calculated from a regression of NEE versus APAR using Equation [6], R_{total} will usually not include wintertime and night carbon exchange measurements, the annual sum will not be an estimate of the amount of carbon sequestered in the soil as organic matter. Instead, the annual sum of autotrophic and heterotrophic respiration can be estimated using phenomenological models.

The chamber measurements of respiration were obtained over the wintertime and nighttime, and hence were used in a regression with daily average temperature. The regression equations of $\ln(\text{rate})$ versus daily average temperature for the two sites were not significantly different, so the data were combined for the final equation (Fig. 3). The slope of the $\ln(\text{rate})$ versus temperature is equivalent to a Q_{10} of 2.2, a reasonable value, although it is somewhat higher than the average Q_{10} of about 2.0 (Raich and Schlesinger 1993).

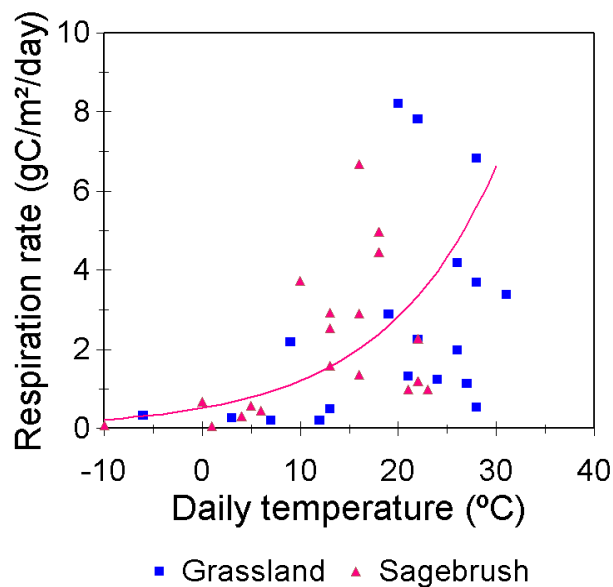


Figure 3. Daily respiration versus average daily air temperature for the grassland and sagebrush sites. Total respiration includes both autotrophic and heterotrophic respiration. The equation of the line is $\exp(0.0783 \text{ temperature} - 1.109)$, with an $R^2 = 0.49$.

Soil moisture is also known to be an important predictor of ecosystem carbon exchange rates, but was not an important variable for these sites. Most of the precipitation at these two sites falls during the spring and summer, when the soils are warm, so there is a large covariance between temperature and soil moisture at these sites. This will not be true for other locations. Furthermore, aboveground living biomass can be an important variable for respiration particularly for forests (Hunt, 1994).

Because respiration was not measured for the forest or the agricultural sites, it is assumed that the respiration response to average daily temperature (Fig. 3) applies to these two sites. Air temperatures (Fig. 1) were used to estimate total respiration for 1999 for each site (Table 2). GPP were obtained as the study-site average (Color Plate 6B). The calculated annual NEE was large and positive sink for the forest and the sagebrush area, whereas the grassland and agricultural sites were close to carbon balance (Table 2).

Table 2 Predicted annual gross primary production (GPP, $\text{g C m}^{-2} \text{ year}^{-1}$), total autotrophic and heterotrophic respiration (R_{total} , $\text{g C m}^{-2} \text{ year}^{-1}$), and net ecosystem exchange (NEE, $\text{g C m}^{-2} \text{ year}^{-1}$) for 1999. Positive NEE are sinks of carbon and negative NEE are sources of carbon to the atmosphere.

Site	GPP	R_{total}	NEE
Grassland	321	307	14
Sagebrush	239	197	42
Agriculture	335	336	-1
Forest	312	257	55

5. DISCUSSION AND CONCLUSIONS

This study did not determine whether all mixed-grass prairie and sagebrush landscapes are in carbon balance or net sinks, respectively, because these predictions were made for specific sites in Wyoming over a specific time period. The source/sink status of the forest and agricultural sites are less certain because respiration rates were not measured for these ecosystems. With newly available climatic data, gridded into GIS layers, a respiration model could be applied to the same aerial extent as the AVHRR data in order to locate potential carbon sources and sinks without the huge number of sites required for a statistically valid inference. The most critical unknown in this proposed methodology is understanding the value of ϵ .

The cool air temperatures in southeastern Wyoming (Fig. 1) are favorable for high quantum yields (Table 1) so a reasonable maximum value of ϵ for gross photosynthesis should be about $3.0 \text{ g C MJ}^{-1} \text{ APAR}$. When the maximum value of ϵ is reduced 50% to account for light saturation (Ruimy et al., 1995), ϵ should be about $1.5 \text{ g C MJ}^{-1} \text{ APAR}$, similar to what was found with only four points at the agricultural site. The difference between 1.5 and the value of 0.51, determined from the aircraft NEE data (Fig. 2), may be attributable to climatic reductions of gross photosynthesis.

Evergreen coniferous forests have little variation in APAR, and have most of the variation in GPP resulting from changes in ϵ (Hunt and Running, 1992). The aircraft flux data were acquired over one year and the chamber flux data were acquired over two years. Therefore, there may be considerable year-to-year variability in ϵ , which was not found in this study. Models such as BIOME-BGC (Hunt and Running, 1992; Running and Hunt, 1993), Glo-PEM (Prince and Goward,

1995; Goetz and Prince, 1999) and 3-PG (Waring et al., 1995; Landsberg and Waring, 1997) could be used to assess variability in ϵ caused by climate.

Alternatively, quantum yield may be determined by measuring leaf fluorescence (Theisen, Chapter 12). Daytime measurements of fluorescence using Fraunhofer lines (Theisen, Chapter 12) presents a new avenue for research which may be applicable for the remote sensing of radiation use efficiency.

However, grasslands and shrublands have very large year-to-year variation in NDVI, depending on precipitation. The typical response of these vegetation types to drought is to senesce, reducing the amount of foliage above ground. Thus, changes in GPP are better represented by changes in APAR rather than changes in ϵ . The value of ϵ can be estimated with NEE data currently available (Svejcar et al., 1997; Frank et al., 2001). Therefore, a map of carbon sources and sinks for rangelands is feasible using the method of combining NEE data with remote sensing presented here. With large areas of the globe covered by rangelands, the potential for carbon sequestration may be significant (Follett et al., 2001).

6. ACKNOWLEDGMENTS

We thank Brian Miyake for assistance of with the AVHRR image processing, Mark McNeal for collection of spectral irradiance and solar irradiance data, and Robert Piper for collection of the chamber flux data. This project was funded by a National Science Foundation grant (IBN-9727796) to the University of Wyoming.

7. REFERENCES

- Asrar, G., M. Fuchs, E.T. Kanemasu, and J.L. Hatfield. 1984. Estimating absorbed photosynthetically active radiation and leaf area index from spectral reflectance in wheat. *Agron. J.* 76:300-306.
- Baldocchi, D., R. Valentini, S. Running, W. Oechel, and R. Dahlman. 1996. Strategies for measuring and modelling carbon dioxide and water vapour fluxes over terrestrial ecosystems. *Glob. Change Biol.* 2:159-168.
- Baret, F., and G. Guyot. 1991. Potentials and limits of vegetation indices for LAI and APAR assessment. *Remote Sens. Environ.* 35:161-173.
- Cihlar, J., H. Ly, Z. Li, J. Chen, H. Pokrant, and F. Huang. 1997. Multitemporal, multichannel AVHRR data sets for land biosphere studies – Artifacts and corrections. *Remote Sens. Environ.* 60:35-57.
- Driese, K.L., W.A. Reiners, E.H. Merrill, and K.G. Gerow. 1997. A digital land cover map of Wyoming, USA: a tool for vegetation analysis. *J. Veg. Sci.* 8:133-146.
- Eidenshink, J.C. 1992. The 1990 Conterminous U. S. AVHRR Data Set. *Photogramm. Eng. Remote Sens.*

Follett, R.F., J.M. Kimble, and R. Lal. 2001. The potential of U.S. grazing lands to sequester soil carbon. *The Potential of U.S. Grazing Lands to Sequester Carbon and Mitigate the Greenhouse Effect*. R.F. Follet, J. M. Kimble, and R. Lal (eds.) Lewis Publishers, Boca Raton, FL. Pp. 401-430.

Frank, A.B., P.L. Sims, J.A. Bradford, P.C. Mielnick, W.A. Dugas, and H.S. Mayeux. 2001. Carbon dioxide fluxes over three Great Plains grasslands. *The Potential of U.S. Grazing Lands to Sequester Carbon and Mitigate the Greenhouse Effect*. R.F. Follet, J. M. Kimble, and R. Lal (eds.) Lewis Publishers, Boca Raton, FL. Pp. 167-187.

Goetz, S.J., and S.D. Prince. 1999. Modelling terrestrial carbon exchange and storage: Evidence and implications of functional convergence in light-use efficiency. *Adv. Ecol. Res.* 28:57-92.

Goulden, M.L., J.W. Munger, S.M. Fan, B.C. Daube, and S.C. Wofsy. 1996. Measurements of carbon sequestration by long-term eddy covariance: methods and a critical evaluation of accuracy. *Glob. Change Biol.* 2:169-182.

Goward, S.N., and K.F. Huemmrich. 1992. Vegetation canopy IPAR absorptance and the normalized difference vegetation index: An assessment using the SAIL model. *Remote Sens. Environ.* 39:119-140.

Gower, S.T., C.J. Kucharik, and J.M. Norman. 1999. Direct and indirect estimation of leaf area index, f_{apar} , and net primary production of terrestrial ecosystems. *Remote Sens. Environ.* 70:29-51.

Gutman, G.G. 1991. Vegetation indices from AVHRR: An update and future prospects. *Remote Sens. Environ.* 35:121-136.

Gutman, G.G. 1999. On the use of long-term global data of land reflectances and vegetation indices derived from the Advanced Very High Resolution Radiometer. *J. Geophys. Res.* 104:6241-6255.

Hanson, P.J., N.T. Edwards, C.T. Garten, and J.A. Andrews. 2000. Separating root and soil microbial contributions to soil respiration: A review of methods and observations. *Biogeochemistry* 48:115-146.

Hunt, E.R., Jr. 1994. Relationship between woody biomass and PAR conversion efficiency for estimating net primary production from NDVI. *Int. J. Remote Sens.* 15:1725-1730.

Hunt, E.R., Jr., and S.W. Running. 1992. Simulated dry matter yields for aspen and spruce stands in the North American boreal forest. *Can. J. Remote Sens.* 18:126-133.

Kelly, R.D., E.R. Hunt, Jr., W.A. Reiners, W.K. Smith, and J.M. Welker. 2002. Correlations of daytime carbon dioxide flux with remotely-sensed vegetation index for four different mountain/plains ecosystems. *J. Geophys. Res.* 107(D14):19.1-19.8.

Landsberg, J.J., and R.H. Waring, 1997. A generalised model of forest productivity using simplified concepts of radiation-use efficiency, carbon balance and partitioning. *For. Ecol. Manag.* 95:209-228.

Myneni, R.B., and D.L. Williams. 1994. On the relationship between FAPAR and NDVI. *Remote Sens. Environ.* 49:200-211.

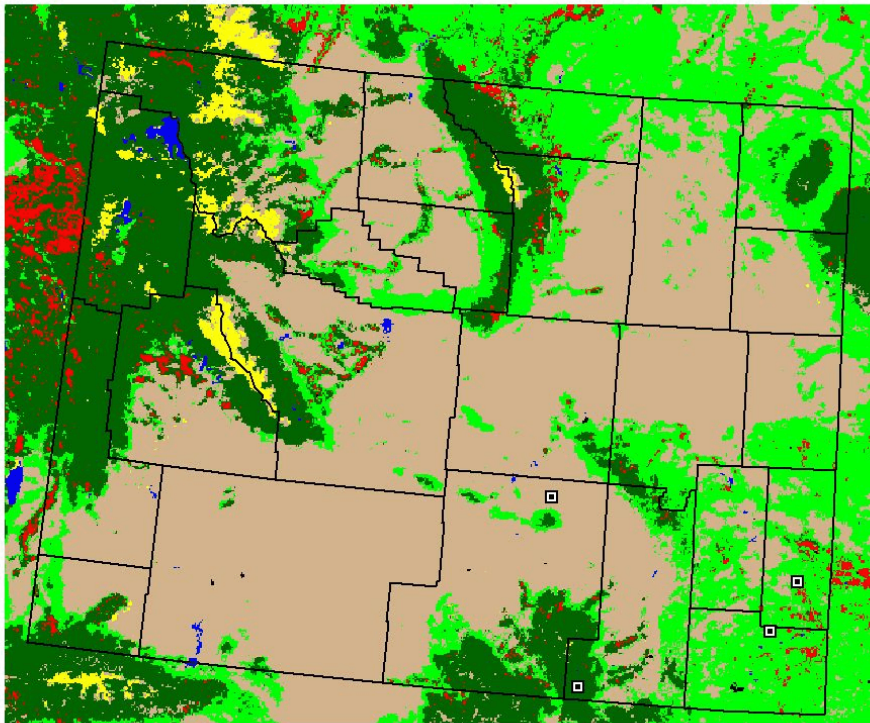
Paustian, K., C.V. Cole, D. Sauerbeck, and N. Sampson. 1998. CO₂ mitigation by agriculture: An overview. *Clim. Change* 40:135-162.

- Prince, S.D. 1991. A model of regional primary production for use with coarse resolution satellite data. *Int. J. Remote Sens.* 12:1313-1330.
- Prince, S.D., and S.N. Goward. 1995. Global primary production: a remote sensing approach. *J. Biogeogr.* 22:815-835.
- Raich, J.W., and W.H. Schlesinger. 1993. The global carbon dioxide flux in soil respiration and its relationship to vegetation and climate. *Tellus B*44:81-99.
- Rouse, J.W., R.H. Haas, J.A. Schell, and D.W. Deering. 1974. Monitoring vegetation systems in the Great Plains with ERTS. Third Earth Resources Technology Satellite-1 Symposium. Volume I: Technical Presentations. S.C. Freden, E.P. Mercanti, M. Becker (eds.) NASA SP-351, National Aeronautics and Space Administration, Washington, D.C. Pp. 309-317.
- Ruimy, A., G. Dedieu, and B. Saugier. 1994. Methodology for the estimation of terrestrial net primary production from remotely sensed data. *J. Geophys. Res.* 99:5263-5283.
- Ruimy, A., P.G. Jarvis, D.D. Baldocchi, and B. Saugier. 1995. CO₂ fluxes over plant canopies and solar radiation: A review. *Adv. Ecol. Res.* 26:1-66.
- Ruimy, A., L. Kergoat, C.B. Field, and B. Saugier. 1996. The use of CO₂ flux measurements in models of the global terrestrial carbon budget. *Glob. Change Biol.* 2:287-296.
- Running, S.W., and E.R. Hunt, Jr. 1993. Generalization of a forest ecosystem process model for other biomes, BIOME-BGC, and an application for global-scale models. *Scaling Physiological Processes: Leaf to Globe.* J.R. Ehleringer and C. Field (eds.). Academic Press, San Diego. Pp. 141-158.
- Running, S.W., D.D. Baldocchi, D.P. Turner, S.T. Gower, P.S. Bakwin, and K.A. Hibbard. 1999. A global terrestrial monitoring network integrating tower fluxes, flask sampling, ecosystem modeling and EOS satellite data. *Remote Sens. Environ.* 70:108-127.
- Sinclair, T.R., and T. Horie. 1989. Leaf nitrogen, photosynthesis, and crop radiation use efficiency: a review. *Crop Sci.* 29:90-98.
- Sinclair, T.R., and R.C. Muchow. 1999. Radiation use efficiency. *Adv. Agron.* 65:215-265.
- Svejcar, T., H. Mayeux, and R. Angell. 1997. The rangeland carbon dioxide flux project. *Rangelands* 19:16-18.
- Theisen, A. F. (2002). Detecting chlorophyll fluorescence from orbit: the Fraunhofer line depth model. From Laboratory Spectroscopy to Remotely Sensed Spectra of Terrestrial Ecosystems. R. S. Muttiah (ed.). Kluwer Academic Publishers, Dordrecht, Netherlands. Pp. 203-232.
- Waring, R.H., B.E. Law, M.L. Goulden, S.L. Bassow, R.W. McCreight, S.C. Wofsy, and F.A. Bazzaz. 1995. Scaling gross ecosystem production at Harvard Forest with remote sensing: a comparison of estimates from a constrained quantum-use efficiency model and eddy correlation. *Plant Cell Environ.* 18:1201-1213.
- Winslow, J.C., E.R. Hunt, Jr., and S.C. Piper. 2001. Models of solar irradiance based on daily humidity, precipitation and temperature data for various spatial scales and global-change applications. *Ecol. Modell.* 143:227-243.

8. ABBREVIATIONS AND SYMBOLS

APAR	Absorbed photosynthetically active radiation ($\text{MJ m}^{-2} \text{ day}^{-1}$ or W m^{-2}) from 400 nm to 700 nm wavelength
AVHRR	Advanced Very High Resolution Radiometer
f_{APAR}	Fraction of the incident photosynthetically active radiation that is absorbed by vegetation
GIS	Geographic Information Systems
GPP	Gross primary production ($\text{g C m}^{-2} \text{ time}^{-1}$)
NDVI	Normalized difference vegetation index
NEE	Net ecosystem exchange ($\text{g C m}^{-2} \text{ time}^{-1}$)
PAR	Incident photosynthetically active radiation ($\text{MJ m}^{-2} \text{ day}^{-1}$ or W m^{-2})
R_{total}	Total respiration ($\text{g C m}^{-2} \text{ time}^{-1}$)
ϵ	The efficiency of radiation use ($\text{g C MJ}^{-1} \text{ APAR}$)

Color Plate 6A. Wyoming landcover map and location of four study sites in the southeastern portion of the state. The landcover map was derived from the United States Geological Survey Classification using AVHRR data. The grassland site (lower right) and sagebrush shrubland site (upper left) were studied in detail. Flux data for the mixed agricultural site (upper right) and coniferous forest site (lower left) were not as comprehensive. The colors are: light green - grassland, tan - shrublands, red - agricultural, dark green - forest, yellow - tundra, blue - water, and black - unvegetated/urban. These data were obtained from the EROS Data Center Distributed Active Archive Center (EDC DAAC).



Color Plate 6B. Gross primary production ($\text{g C m}^{-2} \text{ year}^{-1}$) for Wyoming, USA, in 1999 estimated from weekly AVHRR NDVI, landcover class, and meteorological data. The colors are: black - no vegetation, purple - GPP from 0 to 150, dark blue - GPP from 150 to 200, light blue - GPP from 200 to 250, dark green - GPP from 250 to 300, light green - GPP from 300 to 350, orange - GPP from 350 to 400, red - GPP from 400 to 450, white - GPP from 450 to 600.

